Journal of Building Engineering 40 (2021) 102698

Contents lists available at ScienceDirect

Journal of Building Engineering

journal homepage: www.elsevier.com/locate/jobe

Evaluation of EN15193-1 on energy requirements for artificial lighting against Radiance-based DAYSIM

Luka Akimov [a,b,c,*], Giuseppe De Michele [b], Ulrich Filippi Oberegger [b], Vladimir Badenko [a], Andrea Giovanni Mainini [c]

[a] Peter the Great Saint-Petersburg Polytechnic University, 29 Polytechnicheskaya St., St.Petersburg, 195251, Russian Federation
[b] EURAC Research, Institute for Renewable Energy, 1 Viale Druso, Bozen/Bolzano, 39100, Italy
[c] Politecnico di Milano, 32 Piazza Leonardo da Vinci, Milano, 20133, Italy

ARTICLE INFO

Keywords:
DAYSIM
Radiance
EN15193-1:2017
Artificial lighting
Daylight
LENI

ABSTRACT

This study evaluates the calculation approach of the energy requirements for artificial lighting inside buildings of different use according to EN15193-1:2017, defining the main scope of the standard, highlighting its limitations, and proposing improvements. The evaluation was carried out through a parametric analysis to determine the influence of window-to-wall ratio, distribution of windows, presence of side opening, glazing visible transmittance, and overhang length on the calculation of the Lighting Energy Numeric Indicator (LENI) for a living room and an office at four representative locations (Bratislava, Stockholm, London, Athens). The standard was tested against DAYSIM, a Radiance-based simulation tool for calculating daylight availability, whose results were post-processed to obtain the energy requirements for artificial lighting. For many windows close to each other, the standard's approach to superimpose the daylight factors (DF) for overlapping daylit areas led to an overestimated total DF and therefore an underestimated LENI. For rooms with low window-to-facade and window-to-wall ratio, the standard's calculation was inaccurate. The daylight supply factor tabulated in the standard was too low for latitudes below 45°, leading to an overestimation of the LENI. For latitudes above 60°, the opposite effect was observed. Summarising, the standard underestimated the LENI by about 10% on average.

1. Introduction

Lighting in commercial buildings accounts for up to 45% of overall electricity demand, with significant variation from one building to another [1]. In modern office buildings, electric lighting can provide substantial energy savings with the introduction of reasonable investments [2]. For Northern European countries, it has been demonstrated that the transition to energy efficient lighting systems is one of the most effective and economical methods of reducing CO2 emissions both for new and retrofitted buildings [3].

In recent years, tools for lighting simulation in buildings have become a promising and widely-used method by designers for lighting energy analysis in order to identify the most suitable energy saving options [4]. However, their use is challenging because they require a detailed representation of the real environment. This leads to time-consuming model design and long computation time in case of complex geometries [4]. Moreover, setting up simulations requires very specific knowledge, and the user interface may not be user-friendly [4].

The standard EN15193-1:2017 [5] (henceforth referred to as "standard") establishes a calculation method for determining the energy requirements for artificial lighting in buildings. The evaluation is done without creating a comprehensive 3D model of the building, thus permitting fast evaluation during preliminary design. This preliminary information can then be used to inform the actual, detailed design. The main numerical result from the standard is the LENI (Lighting Energy Numerical Indicator), which quantifies the annual energy consumption for lighting per square meter of treated floor area and is typically expressed in kWh/m^2·yr. The detailed calculation method proposed by the standard can be applied for energy certification related to lighting energy consumption of buildings.

The LENI calculation procedure considers, at different levels of detail, the following factors affecting the building's energy consumption for electric lighting: 1) lighting system power, including parasitic power of control systems and power for recharging the emergency lamps; 2) control system type (manual or automatic according to daylight availability, occupancy or both); 3) daylight penetration into the indoor spaces through both vertical glazing and roof lighting systems, which is

* Corresponding author. Peter the Great Saint-Petersburg Polytechnic University, 29 Polytechnicheskaya st., St.Petersburg, 195251, Russian Federation.
E-mail addresses: lukakimov@gmail.com, akimov.li@edu.spbstu.ru (L. Akimov).

https://doi.org/10.1016/j.jobe.2021.102698
Received 14 January 2021; Received in revised form 1 April 2021; Accepted 6 May 2021
Available online 16 May 2021

List of notations

LENI	Lighting Energy Numerical Indicator [kWh/m^2·yr]
WWR	Window to Wall Ratio
WFR	Window to Floor Ratio
DF	Daylight Factor
$W_{L,t}$	Estimated lighting energy required to provide a zone of the building with adequate illumination [kWh/year]
$W_{P,t}$	Estimated standby energy required during periods in which lighting is switched off to provide the charging energy for emergency lighting and activation energy for lighting controls in a zone of the building [kWh/year]
W	Total annual energy consumption for lighting in the building [kWh/year]
F_D	Daylight dependency factor
$F_{D,S,j}$	Daylight supply factor of surface j
$F_{D,S,SNA,j}$	Daylight supply factor of surface j evaluated whenever the solar protection system is inactive
$F_{D,S,SA,j}$	Daylight supply factor of the area j evaluated whenever the solar protection system is active
γ	Site latitude
t_D	Daylight time [hours]
t_N	Daylight absence time [hours]
P_n	Budget power installed [W]
F_c	Constant illuminance dependency factor
F_o	Occupancy dependency factor
P_j	Power density of the lighting [W/m^2]
$P_{j,lx}$	Power density per lux of the area [W/lm]
E_m	Maintained illuminance that the lighting system will be designed to provide [lx]
F_{MF}	Correction factor to account for the maintenance factor MF that is used in the lighting system design
MF	Maintenance factor
F_{CA}	Factor to account for the reduced power required if parts of the area are lit to a lower level, it equals to 1 if the full illuminance is required for the whole area
F_L	Correction factor to account for the efficiency of the lighting equipment that will be used in the lighting system
H_{dir}/H_{glob}	Luminance exposure, ratio between direct (H_{dir}) and global (H_{glob}) illuminances calculated on the horizontal plane
F_c	Constant illuminance dependency factor
$t_{rel,D,SNA,j}$	Relative portion of the total operating time during which the solar protection system is inactive
$t_{rel,D,SA,j}$	Relative portion of the total operating time during which the solar protection system is active
F_L	Light source efficiency factor
$D_{CA,j}$	Faylight factor of the raw carcass opening
$I_{Tr,j}$	Transparency index
A_{Ca}	Area of raw building carcass opening [m^2]
A_D	Daylit area (i.e., the area exposed to daylight) [m^2]
$I_{RD,j}$	Space depth index
$I_{Sh,j}$	Shading index
$F_{D,C}$	Correction factor for daylight responsive control
ab	Ambient bounces
lw	Limit weight
aa	Ambient accuracy
ad	Ambient divisions
ar	Ambient resolution
DA_500	Daylight Autonomy with a threshold of 500 lux
ρ_F	Floor surface reflectance
ρ_W	Walls surface reflectance
ρc	Ceiling surface reflectance
ρ_F	External overhang surface reflectance

a function of window-to-wall ratio (WWR), facade window distribution, and glazing visible transmittance; 4) building usage and corresponding lighting requirements, including occupancy time and probability [5].

There are several studies based on the standard's methodology of estimating the annual energy consumption for lighting. For example, in Ref. [6] the authors critically discuss the procedure prescribed by the Italian Technical Standards to account for the internal gains in the calculation of the energy performance indices for a building. The paper proposes a new procedure, which relies on the lighting energy numerical indicator (LENI) according to the European Standard EN 15193:2007. The papers [7–21] use the approach incorporated in earlier versions of the standard – either EN15193-1:2007 or prEN 15193-1:2015 – in the conducted tests evaluating daylight availability, energy efficiency and economic benefits from saving potential associated with artificial light energy use. Lo Verso et al. [22,23] present the results of a study quantifying, concerning a manual on/off switch, the energy savings due to the four typologies of daylight-linked controls included in the latest revision of the standard as well as their combination with an occupancy automatic off control. The results show for what combinations of variables two target savings of 20% and 30% can be reached using the photo dimming and occupancy controls contained in the standard.

From the discussed literature, it can be concluded that the standard's calculation approach is highly recognized and widely used by designers and researchers as the ground truth in the annual energy consumption associated with artificial lighting estimation. For instance, the standard's LENI calculation is included in the software Dialux used for professional light design by designers and manufacturers [24]. The new software LENICALC, developed by ENEA and available since February 2020, calculates the LENI indicator trying to follow the standard as strictly as possible while guiding the user in setting each required parameter [25].

Nevertheless, few studies exist that compare the standard to more accurate methods [26–33], and most works are related to the previous version of the standard. A major change to the standard's calculation method has been the process of daylight availability estimation [34]. The new version of the standard has been evaluated in Ref. [35] in which, based on 108 cases, the authors compared the calculation of the daylight factor (DF) according to the current version of the standard against DAYSIM. The results of the study showed a very good correlation (R2 = 0.99). However, only a single window was included in the model and the case of multiple openings providing daylight to space was not considered. Additionally, the LENI was evaluated for few of the considered cases, and mainly for comparing different lighting control.

Therefore, to better understand the limitations and scope of applicability of the standard, it is necessary to extend the comparisons done in previous studies by considering cases that include important, unevaluated factors, such as a broader range of latitudes, different window-to-floor and window-to-wall ratios (WFR and WWR, respectively), and multiple windows.

This paper provides an assessment of the standard's energy requirements calculation in terms of LENI and DF respectively against DAYSIM [36] and Radiance [37], by performing a parametric analysis that considers, in addition to the evaluation in Ref. [35], the impact of the following crucial factors in the calculation of the LENI: window-to-wall ratio, distribution of windows, presence of side opening, glazing visible transmittance, overhang length, space geometry, and room location. Such an evaluation is important because the new version substantially revised the daylight availability calculation, which has a

strong impact on the LENI and therefore on lighting design in buildings. The influence of the above-mentioned factors is in-deep investigated and weaknesses and limitations of the current version of the standard are identified and demonstrated. Finally, suggestions for possible improvements of the standard are given.

2. Overview of the standard [5]

Fig. 1 represents a flow chart of the steps proposed by the standard to obtain the LENI:

Accordingly, the standard's calculation procedure can be divided into the following steps.

- **Zone under evaluation:** definition of its geometry and use;
- **Estimation of installed electric power** from the luminaire types installed in the zone;
- **Definition of the luminaire control system**;
- **Daylight availability estimation** from location (latitude) façade's orientation, weather data, openings geometry, glazing properties, and shading systems. Daylight availability is a function of daylight factor (DF) calculated by the approach within the areas exposed to daylight;
- **Result**: total energy use and the LENI are calculated. They consider daylight availability and are defined as minimum required electric energy for artificial lighting to meet adequate internal illuminance levels.

The main parameter constituting the LENI is the estimated lighting energy $W_{L,t}$ required to provide a zone of the building with adequate illumination. It is defined by Eq. (A2) reported in the Appendix. $W_{L,t}$, among other factors, is a function of the daylight dependency factor F_D defined by Eq. (A.6). F_D depends on building location and geometry along with openings geometry, obstructions presence, shading device presence/absence and glazing properties.

One of our goals was to compare daylight availability calculated according to the standard with a calculation in DAYSIM. We did not evaluate the need for solar shading activation due to glare. Therefore, we neglected the factor called "solar/glare protection activation" [5], accounting for glare protection (see Eq. (A.9)), i.e., we assumed no internal shading. Thus, Eq. (A.9) becomes:

$$F_{D,S,j} = F_{D,S,SNA,j} \tag{2.1}$$

$F_{D,S,SNA,j}$ denotes the daylight supply factor of surface j evaluated whenever the solar protection system is inactive. It is a function of the site latitude γ, the ratio H_{dir}/H_{glob} (so-called luminance exposure) between direct (H_{dir}) and global (H_{glob}) illuminances calculated on the horizontal plane, façade orientation, level of maintained illuminance (E_m) and DF [5]. The daylight supply factor $F_{D,S,SNA,j}$ is a tabular value in the standard.

3. Evaluation method

The evaluation is based on the parameters that constitute the calculation steps defined by the standard.

3.1. Parametric analysis

The main changes made in the standard's recent revision [32] concern the process of daylight availability estimation within the energy assessment. Therefore, we focused ourselves on parameters regarding the standard's calculation of daylight availability, which are essential for calculating the LENI.

In order to estimate the energy use for artificial lighting, the standard derives a quantity termed "daylight factor" (DF) that accounts only for areas exposed to daylight. However, the commonly accepted definition of the DF (see, e.g., Ref. [38]) is different, because it is evaluated on a different reference area, as discussed in Section 3.4. Therefore, we also investigated the appropriateness of the DF calculation as per standard with the use of Radiance because it is essential for understanding the reasons for differences in the LENI results compared with DAYSIM.

Accordingly, the factors chosen for the parametrical analysis are:

3.1.1. Building location

We considered the four locations Athens [GR], Bratislava [SK], Stockholm [SE], London [GB] because the standard provides tables for these locations and to assess whether the accuracy of the results depends on the climatic zone. Table A.1 shows the geographical information and luminous exposure H_{dir}/H_{glob} of the locations. Building location influences the LENI, but not the DF calculation.

3.1.2. Room dimensions

Two different room dimensions were chosen based on the sample geometries from Refs. [39,40]. The dimensions are listed in Table 1.

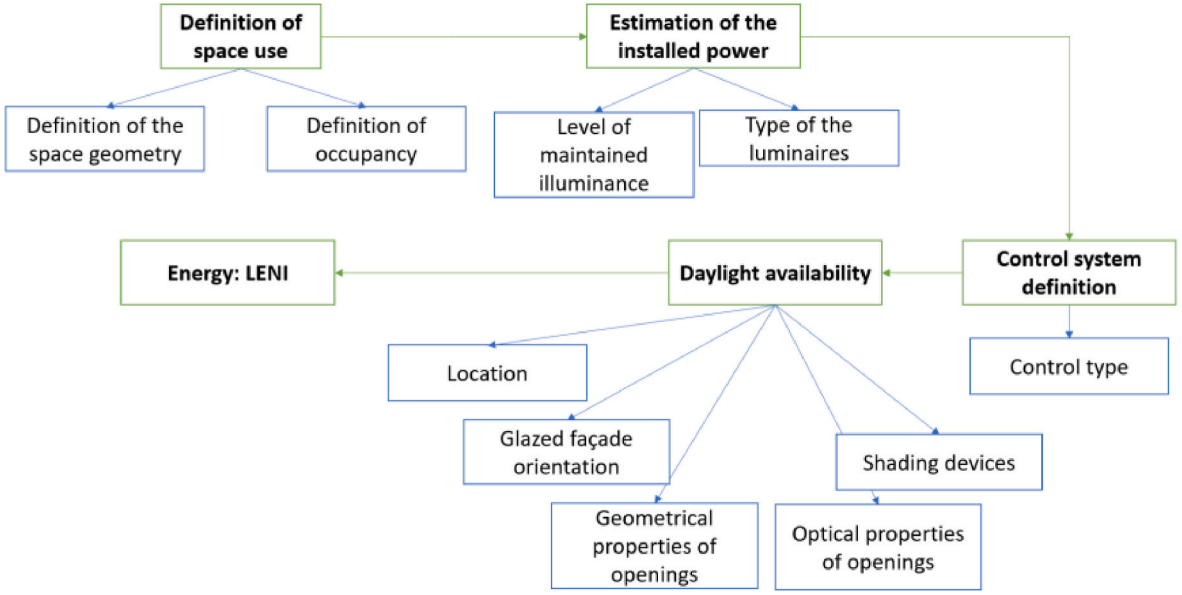

Fig. 1. Flow chart of the steps for calculation of the LENI with use of methodology based on the EN15193-1:2017 calculation approach.

Table 1
Room geometries.

Building use	Length [m]	Depth [m]	Height [m]
Residential (living room)	5.5	4.5	2.7
Office	8.45	8.45	3.3

The dimensions in Table 1 refer to the centerline of the walls. Since within the standard approach the thickness of elements that constitutes the zone is neglected, in our simulations, the walls, floor and ceiling were modeled with zero thickness.

Both the living room and the office are south-oriented, meaning that the window openings are located on the south façade for both building uses.

Zone geometry influences the daylit area and therefore affects both the DF and the LENI calculation.

3.1.3. South facade window-to-wall ratio

The window-to-wall ratio (WWR) is parameterized by window height and sill level above the floor as shown in Table 2:

The current version of the standard does not explicitly consider the window frame. In the standard, WWR is understood as the transparent (glazing) over the opaque (including the window frame) part of the façade. Therefore, we modeled all windows in DAYSIM and Radiance without a frame to be compliant with standard's WWR definition in our analysis.

WWR is in direct relation with WFR (window-to-floor ratio), which is the ratio between the transparent window area (glazing) over the analyzed space floor area. The dependence between WWR and WFR for the geometries that we used for our analysis is shown in Table 3:

3.1.4. Window presence on the west façade

Two options were considered: either there is no window on the west façade, or there is a single opening with WWR = 0.2. This parameter is introduced to analyze how the presence of side windows influences the DF and energy use.

3.1.5. Number of windows on the south façade

For fixed WWR of the south façade, sill level above floor and window height, increasing the number of windows reduces the width of each window. This changes the distribution of light coming from the façade and influences the DF and the LENI.

For the living room we considered 1, 2, 3 or 6 windows on the south façade for every value of WWR, while the office has 2, 3, 4 or 8 windows in case of WWR 0.1 or 0.3 and only one window for a WWR of 0.5 or 0.7.

Fig. 2 shows for the office and a fixed WWR of 0.1 how the south facade window distribution changes with an increase of the number of windows.

3.1.6. Glazing visible transmittance

Double and triple glazings were simulated with a visible transmittance of 0.73 and 0.63, respectively [41].

3.1.7. Horizontal overhang presence

The presence of an overhang in the calculation of the standard influences light penetration and affects energy consumption.

Three different depths for the horizontal overhang were tested: 0.2, 0.4 and 0.6 m. The overhang was placed at the upper edge of the window glazing. The case without overhang has also been considered.

Table 2
WWR on the south facade.

WWR, south facade	Window height [m]	Sill level above the floor [m]
0.1	1	0.9
0.3	1.25	0.9
0.5	1.5	0.9
0.7	2.2	0.2

Table 3
WWR and WFR dependence.

WWR	Windows area	WFR	Windows area	WFR
	Living room (floor area = 24.75 m^2)		Office (floor area = 71.4 m^2)	
0.1	1.485	0.060	2.788	0.039
0.3	4.455	0.180	8.366	0.117
0.5	7.425	0.300	13.943	0.195
0.7	10.395	0.420	19.520	0.273

WWR influences the daylit area and therefore affects both the DF and the LENI calculation.

3.2. Design of experiment

We performed two full factorial analyses, one for the DF and one for the LENI, using the factors listed in Section 3.1.

As already mentioned, the DF estimation as per standard was compared with Radiance results because the LENI calculation in the standard depends on the DF.

Since the DF is independent of building location and window orientation, the full factorial design is given by (levels in parentheses): building geometry (2), south façade WWR (4), number of south facade windows (4), visible transmittance (2 – double and triple glazed systems), overhang length (4), for a total of 256 cases. However, for the office geometry and a WWR of 0.5 and 0.7 there is only one choice regarding the number of windows (see Section 3.1), which reduces the number of simulations to 208.

Fig. 3 shows the parameterization tree used to assess the DF results:

The LENI parameterization includes additional factors such as location (4) and presence (or absence) of the side opening (2). The total number of simulations for the LENI estimation is thus equal to 1668.

Fig. 4 shows the parametrization tree for the assessment of the LENI estimation:

Table 4shows two renders as an example of modeled geometries:

In our analysis we used fixed values of reflectance factors for each surface, Table 5. We did not include reflectance factors in the parametric study because in the standard they occur in the calculation of the Maintenance Factor (MF) through the Room Surface Maintenance Factor (RSMF), together with three other parameters: Lamp Lumen Maintenance Factor (LLMF), Lamp Survival Factor (LSF) and Luminaire Maintenance Factor (LMF). Nevertheless, due to the complexity in deriving MF by means of the various parameters combination, the standard suggests exemplary values, that were used in our analysis.

3.3. Task plane, luminaries and control system

The height of the task plane is fixed at 0.8 m above the floor level, which is assumed to be the height of the working desk in Ref. [5].

The luminaire chosen for all calculations is an LED lamp with a constant illuminance dependency factor $F_c = 0.85$, a maintenance factor MF = 0.7, and a light source efficiency factor $F_L = 0.86$ [5]. The luminaires were set at the ceiling level for both geometries, which is 2.5 m above the task plane for the office and 1.9 m – for the living room. Upward flux fraction was set to 30%. Following the Eq. (A.3) the lighting power densities were calculated: 14.09 W/m^2 for office and 15.59 W/m^2 for the living room.

Daylight responsive control as modeled in the standard considers imperfections of control systems, such as time lags for the activation and deactivation of lighting, inaccuracies in measuring the illuminance level, and manual lighting control by the occupants. However, the standard is not explicit enough about these imperfections to allow for implementation in simulation software. Therefore, we decided to simulate only a simple control logic that assumes that lighting is on if the

Fig. 2. Office south facade for WWR = 0.1 and a varying number of windows.

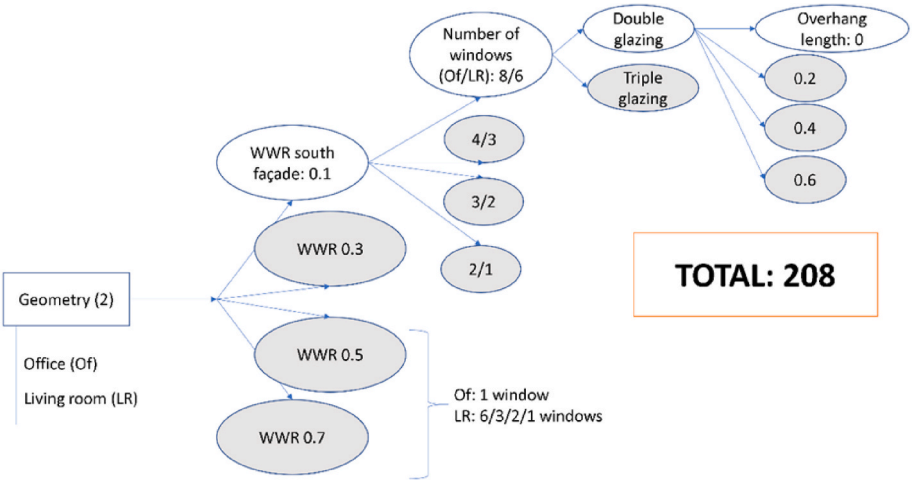

Fig. 3. Parameterization tree for assessing DF estimation.

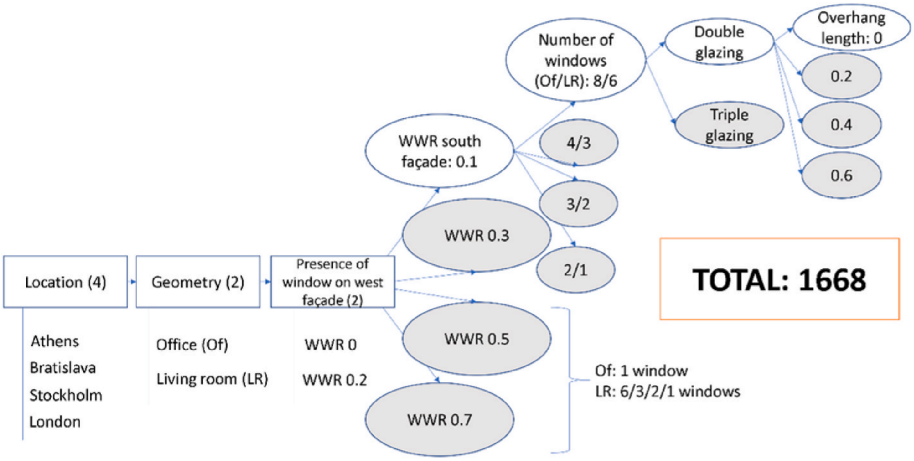

Fig. 4. Parameterization tree for assessing the LENI estimation.

daylight illuminance on the working plane is below 500 lux, and off otherwise. The 500 lux threshold value was set for both the living room and office geometries.

3.4. Daylight factor assessment

The DF is normally calculated considering the whole area of the room under evaluation [38]. In contrast, the standard proposes a simplified calculation of a quantity termed "daylight factor" that only considers areas exposed to daylight. It is then used for the energy requirements calculation within the [5] approach. This "DF" as per standard should thus not be considered a valid indicator by itself but rather an intermediate result that serves the purpose of classifying a zone by daylight availability and calculating lighting energy requirements.

The DF (as per standard) on a floor patch is equal to the sum of the DFs where daylit areas overlap [41] (see Fig. 5).

The overall DF (as per standard) for the total daylit area of the zone is found as a sum of weighted averages of the DFs for each daylit floor patch. The weight is given as a daylit floor patch area divided by the total daylit area. Eq. (3.1) demonstrates the calculation of the final daylight factor of the zone as per standard.

$$DF_{final} = \sum \left(DF_i \times \frac{A_i}{A_{tot}} \right) \tag{3.1}$$

Here, DF_i is the daylight factor calculated on the single daylit area A_i.

Each single daylit area A_i is estimated as:

Table 4
Example renders of a living room and office configuration.

Living room: side opening, south facade WWR = 0.1, 6 windows, overhang depth = 0.2 m	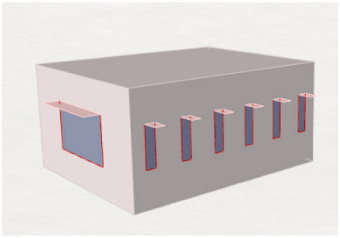
Office: no side opening, south facade WWR = 0.3, 4 windows, no overhang	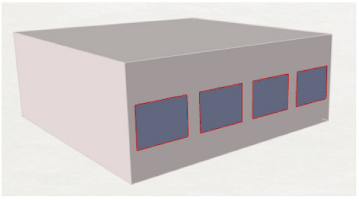

Table 5
Reflectance factors of the surfaces.

Surface	Reflectance factor
Wall	0.5
Ceiling	0.7
Floor	0.2
Overhang	0.1

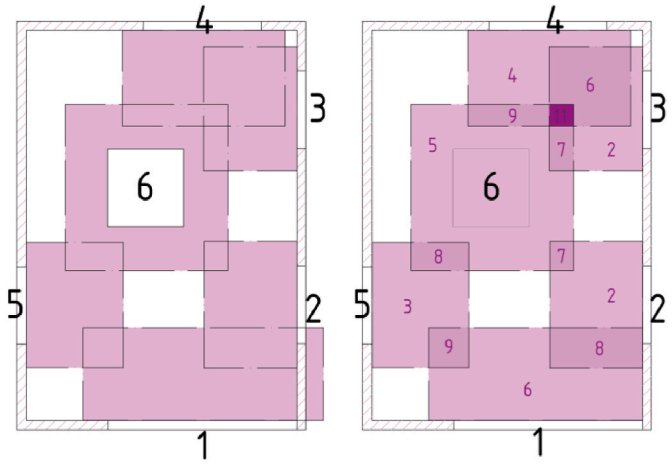

Fig. 5. DF calculation as per standard for overlapping areas: daylit areas cast by the transparent façade elements (left) and superposition of the DFs if daylit areas intersect (right); e.g., DF from opening 3: 2, DF from opening 4: 4, the intersection of daylit areas from openings 3 and 4: 2 + 4 = 6 [41].

$$A_i = a_d \times \left(w + \frac{1}{2}a_d\right) \tag{3.2}$$

Where *w* is the width of the window [m] and a_d is the depth of the daylit area [m] (see Fig. 6).

We used a sweep line algorithm to calculate the total daylit area [42].

3.5. Software used to evaluate the standard

As a reference for the standard evaluation, the Radiance-based software DAYSIM v4 [6] was used. DAYSIM is a validated [36,43] and highly recognized by professionals software in the field of daylighting design and verification [4].

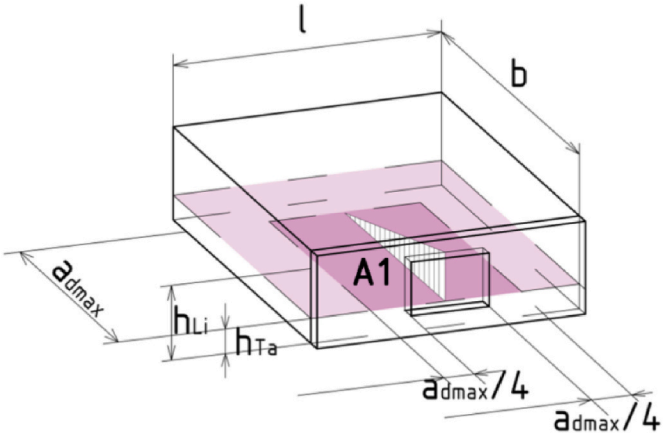

Fig. 6. Estimation of single daylit area with maximum depth a_{dmax}, window lintel height h_{Li} [m] and task area height h_{Ta} [m] [41].

DAYSIM calculation is based on the daylighting coefficient method [44], which allows to carry out a fast annual daylighting simulation. DAYSIM uses the records of direct normal and diffused horizontal irradiances and feeds them into the Perez All-Weather model [45], which is composed of a model that derives illuminance values from irradiances and models that recreate a luminance distribution on the sky vault from illuminance values [46]. The "Interpolated method" of DAYSIM was used in the standard's evaluation [47].

Radiance (version 5.2.1) [7] was used to obtain the DF data. Radiance is a suite of programs for the analysis and visualization of lighting in design [4] that is highly recognized among designers and researchers.

Grasshopper (version 1.0.0007 04/11/2018) [48], a graphical algorithm editor integrated with the 3D modeling tools of Rhino (version 6 SR10: 6.10.18308.14011 11/04/2018) [49], was used to setup the parametrical model.

Within Grasshopper, the plug-ins Honeybee (version 0/0/63 22/01/2018) and Ladybug (version 0/0/6622/01/2018) [50] were used. Honeybee connects Grasshopper to EnergyPlus [51], DAYSIM [36], Radiance [37] and OpenStudio [52] for building energy and daylighting simulations.

The annual energy use for artificial lighting was derived from illuminances using a Python v3.7.1 [53] script for post-processing. The script is described in Section 3.6.

3.6. DAYSIM model definition

Test points for illuminance estimation were generated on the workplane situated at 0.8 m height [5]. The plane was split into a grid with 0.6 by 0.6 m spacing, thus generating 196 sensor points for the office (8.45 m × 8.45 m) and 63 sensor points for the living room (4.5 m × 5.5 m).

The DAYSIM ambient parameters set for the case studies are listed in Table 6.

Given the complexity of the parametrization, to define the most appropriate DAYSIM parameters for performing fast and accurate simulations, a converge test was performed. The test focused on two parameters: ab (ambient bounces) and lw (limit weight), while aa (ambient accuracy), ad (ambient divisions) and ar (ambient resolution) were set to be accurate [54]. A detailed explanation of the effect of the parameters is reported in Ref. [55].

Table 6
Radiance ambient parameters set in the experiment.

ab	aa	ad	ar	lw
5	0.1	2048	300	0.01

The convergence test was performed considering the following indicators: the LENI and average Daylight Autonomy with a threshold of 500 lux (DA_500) [56]. We considered an example case with the following parameters: location Bratislava, office (corresponding schedule described below), WWR 0.5 on south-facing façade with 1 window, side opening on the west facing façade, triple glazing, no overhang.

Figs. 7 and 8 show the effects of different combination of -ab and -lw on the calculation of the LENI and DA_500.

Results show that from ab from 5 to 8 the LENI and DA_500 remain stable. Comparing the results for the two -lw settings, it can be observed that the LENI and DA_500 output are similar. Therefore, ab was set to 5 and -lw to 0.01.

We assumed that the luminaires were fully switched on (no dimming) if the average daylight illuminance inside the test room was below the established 500 lx.

The use schedules were set as follows.

- Office: Mo–Fr 8:00–17:00 (Saturday-Sunday omitted) [5];
- Residential building (living room): Mo-Su 7:00–23:00 [57].

Our Python script extracts illuminances within these schedules and applies the following condition: if the mean daylight illuminance calculated on the task area (0.8 m above the floor level) is lower than 500 lx, artificial light is turned on. By doing this, we obtain the annual number of hours when the artificial light is on.

According to Eq. (A.5), the LENI is affected by daylight time t_D when lighting could be used and daylight absence time t_N. These parameters depend on the latitude, and their calculation procedure is provided by the standard. Knowing the schedule, t_D and t_N were calculated from weather data [51] using a custom-made Python script. Any hour with an illuminance greater than zero was considered daylight time, otherwise daylight absence time. The data is listed in Table 7 and was used in both the DAYSIM and EN15193-1:2017 models.

The light power density, reported in Section 3.3 was used for both the DAYSIM and EN15193-1:2017 models.

Finally, the LENI [kWh/m^2·yr] was calculated by multiplying the lighting power density [W/m^2] by the number of hours when lighting is on.

4. Results and discussion

Results are subdivided according to the parametrization trees for DF and the LENI estimation (see Section 3.2).

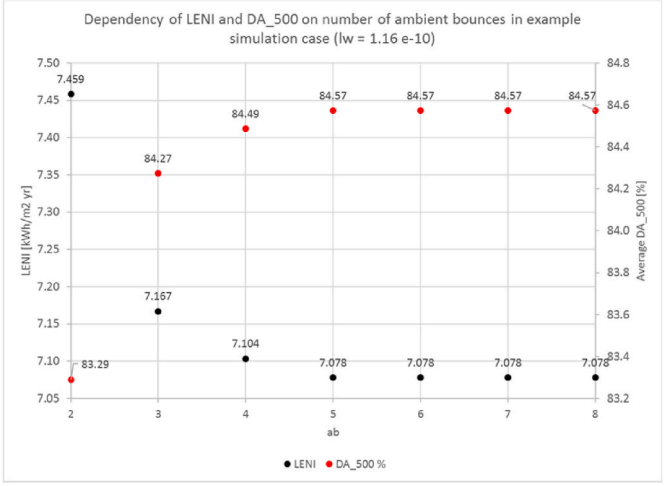

Fig. 7. Dependency of the LENI and DA_500 on -ab in our example case, -lw is set to $1.16 \cdot 10^{-10}$.

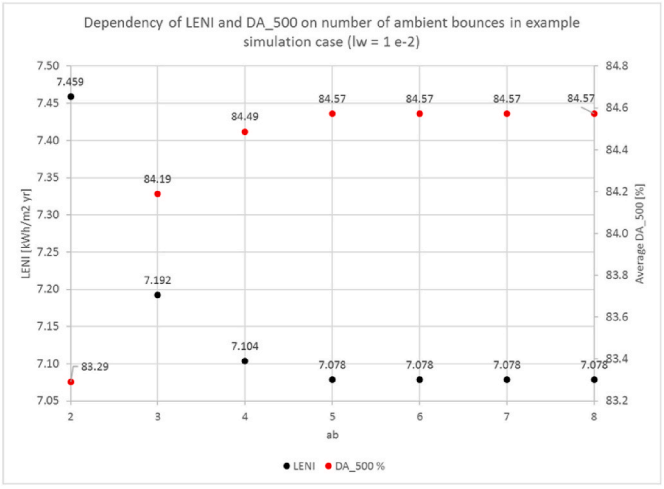

Fig. 8. Dependency of the LENI and DA_500 on -ab in our example case, -lw is set to 0.01.

Table 7
Daylight times and daylight absence times used in the analysis.

Location	Geometry	Daylight time (hours)	Daylight absence time (hours)
Athens [GR]	Office	2340	0
	Living room	4261	1579
Stockholm [SE]	Office	2184	156
	Living room	3877	1963
London [GB]	Office	2292	48
	Living room	4011	1829
Bratislava [SK]	Office	2291	49
	Living room	4002	1838

4.1. DF evaluation

As discussed in Section 3.4, in the approach for the LENI calculation adopted by the standard, the DF is estimated only on areas exposed to daylight. This is different from the conventional way of calculating the DF [38] where the DF is estimated on the whole floor area. To be consistent with the DF estimation as per standard, we evaluated with Radiance considering only daylit areas.

Fig. 9 summarizes the results. Before analyzing the details, we first explain how to read this figure and the following results figures. On the x-axis, the simulation number (index) is shown. The DF (in later figures, the LENI) is plotted on the y-axis. Each figure refers either to the office or the living room. In line with the parameterization for the DF estimation shown in Fig. 3, each graph can be subdivided into four groups according to the variation of the south facade WWR. Each WWR group can be subdivided into four groups representing a different number of windows on the south façade. Each such group can be subdivided further into two subgroups for two levels of visible transmittance that each contains four single results, one for each level of overhang length (including length zero for the cases without overhang).

The figure title indicates the room type (office or living room) and the WWR on the west facade (zero if there is no window on the west facade).

The largest differences between the standard and Radiance results are found for the south WWR 0.7.

From south WWR 0.5 to 0.7, Radiance results change slightly whereas there is a significant increase in DF as per the calculation of the standard.

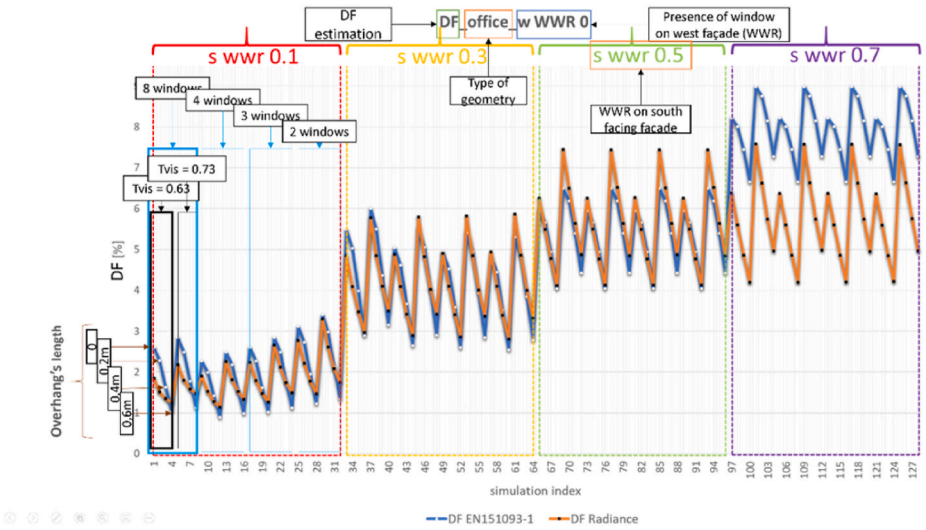

Fig. 9. Explanation of how to read the results figures. This figure shows the results of the DF evaluation for the office without windows on the west facade.

This divergence can be explained by the fact that in both geometries (office and living room), changing the south WWR from 0.5 to 0.7 and keeping the same number of windows, the height of the windows remains the same. The only parameter that changes is the windowsill level, as illustrated in Fig. 10.

Since the height of the task plane is the same for all simulations, the amount of perceived light on the task plane estimated by Radiance is similar in both cases while, in the DF calculation as per standard the window area is included, see Eqs. (A.6) and (A.7).

If the windowsill is below the task area, only the reflected light by the internal surfaces of the space can additionally increase the illuminance level on the task area. The Radiance results, therefore, make more sense in this case, keeping almost the same illuminance level for both WWR 0.5 and 0.7. For WWR 0.7, the standard overestimates the DF by adding the direct light from the part of the window below the task plane to the illuminance on the task plane. It is done due to the mathematical representation of the standard, since the procedure (Eqs. (A.6) and (A.7)) considers the window area.

Fig. 11 shows another discrepancy for WWR 0.1 and 8 small windows on the south façade.

The numerical values for the DF for the eight windows on the south-facing façade and no overhang (simulations 1 and 5) are reported in the figure. In the case of eight windows, a visible discrepancy in the results appears because daylit areas calculated as per standard overlap and the superposition of DFs from each opening leads to a magnified DF for the whole daylit area in the room (see Section 3.4).

Taking the office simulation with parameters WWR 0.1, 8 windows on the south façade, and no side opening on the west facade as an example (simulation number 5, Fig. 11), 61.46% of the total area of the room consists of overlaps of daylit areas that magnify the overall DF as illustrated in Fig. 12.

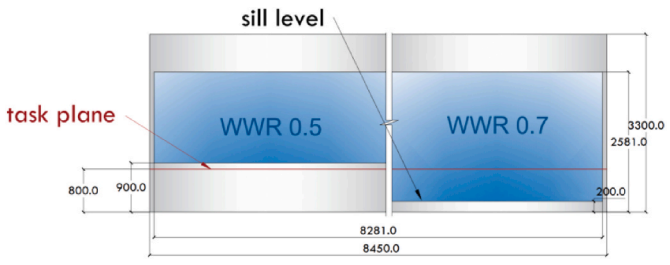

Fig. 10. Change in south façade window geometry from WWR 0.5 (left) to 0.7 (right) for the office.

It is evident from Fig. 12 that the closer window 1 is to window 2, the larger is the overlap area.

To better analyze this dependency between window distribution and overlap of daylit areas, an extreme case is presented in Fig. 13. We kept the facade dimensions as in Fig. 12 and put one window in the middle of the facade with the same width as that of windows 1 and 2 in Fig. 12 joined, which is 0.7 m (twice the width of the window shown in Fig. 12). Its lintel level (height above the floor) is 1.9 m, as illustrated on the left of Fig. 13 (window 1*). The DF for the daylit area cast by light passing through the opening 1*, assuming the same visible transmittance of 0.63 (triple glazing) and no overhang as before, is 2.267 according to the standard. Since there is no other window in this example, this DF is also the DF for the whole daylit area of the room.

Splitting window 1* into two windows of 0.35 m width each with zero distance between them, thus in the same position and of the same total size as window 1*, the configuration on the right of Fig. 13 is obtained.

The DF for the case on the right of Fig. 13 is calculated as per standard as follows:

- Total daylit area (the same as daylit area 1*) is 6.07 m^2 (calculated with a sweep-line algorithm [42]);
- Daylit area from opening 1 is 5.136 m^2 (the same as in simulation no. 5), which results in a weighting coefficient of 5.136/6.07 = 0.846;
- Daylit area and weighting coefficient from opening 2 are the same as for opening 1;
- Overall DF is 1.823 × 0.846 + 1.823 × 0.846 = 3.08 (35% overestimation compared with the case on the left of Fig. 13).

This example demonstrates that the superposition principle proposed by the standard for the evaluation of the overall DF leads to an error in some cases. Possible refinements of this approach should be investigated.

This overestimation of the overall DF leads to an underestimation of the LENI for a high number of windows on the south façade, as shown in Section 4.2.

4.2. LENI evaluation

For easier readability and comparison, the simulations were subdivided into 16 groups according to the parameterization in Fig. 4, i.e. four locations, two room types and the presence or absence of a window on the west facade. In the following sections, each location is analyzed in a separate subsection.

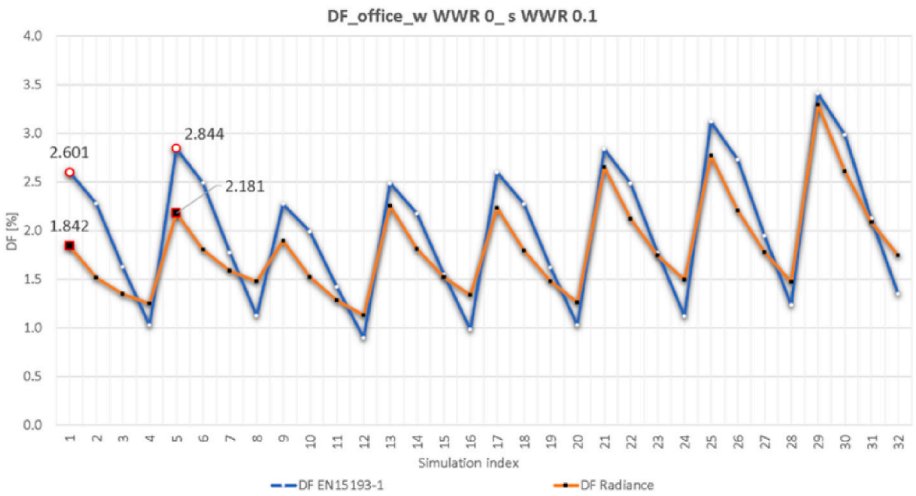

Fig. 11. DF estimation, office, south WWR 0.1, no window on west-facing façade.

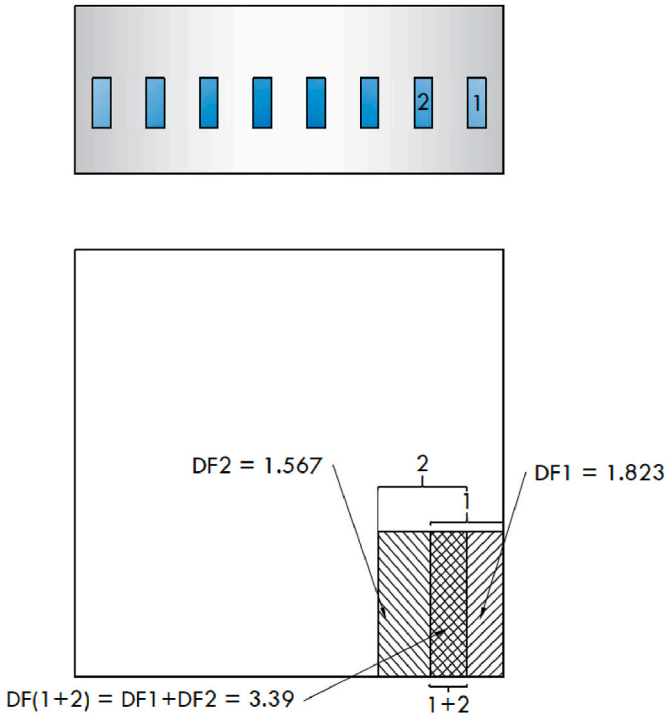

Fig. 12. Superposition of daylit areas, office, south WWR 0.1, 8 windows, triple glazing, overhang length zero.

4.2.1. Athens

Fig. 14 shows the LENI estimation for an office in Athens with a west facade WWR of 0.2.

The calculation as per standard overestimates the LENI significantly in most cases. This is mainly due to the calculation of the daylight supply factor $F_{D,S,j}$ and daylight dependency factor F_D, see Eq. (2.1) and Eq. (A.8), as explained in the following.

According to Eq. (2.1), the daylight supply factor is equal to $F_{D,S,SNA,j}$. This value is tabulated in the standard.

To explain the observed differences, we provide a calculation example for the office geometry with a west facade WWR of 0.2, 8 windows on south-facing façade resulting in a south facade WWR of 0.1, triple glazing and an overhang length of 0.2 m $F_{D,S,SNA,j}$ is tabulated in the standard and parameterized by latitude γ, maintained illuminance E_m, luminous exposure H_{dir}/H_{glob} and DF. The relevant table and ranges for our example are shown in Fig. 15. From Table A.1 we extracted the necessary values for parametrization: location Athens, $\gamma = 37.9°$ and $H_{dir}/H_{glob} = 0.56$. Fixing E_m at 500 lx and considering that the calculated DF of the whole daylit area of the room under investigation was 4.29, we evaluated the $F_{D,S,SNA,j}$ by bilinear interpolation. The ranges of values used in the bilinear interpolation, as highlighted in Fig. 15, were [3,5] for the DF and [0.45, 0.71] for H_{dir}/H_{glob}. This resulted in a value for $F_{D,S,SNA,j}$ of 73.66.

By only changing the location, $F_{D,S,SNA,j}$ varies as reported in Table 8.

Table 8 shows that $F_{D,S,SNA,j}$ is the lowest for Athens. This result is questionable because Athens is the southernmost location in the table and has a hot Mediterranean summer climate (Csa according to the Köppen-Geiger classification) [58], hence it is expected to benefit from more daylight than the other locations. This is confirmed by the luminous exposure, which is the highest for Athens, see Table A.1.

The daylight dependency factor F_D for each location is reported in Table 9. According to Eq. (A.2), the lower the F_D, the lower the estimated energy use for artificial lighting. Therefore, for Athens ($F_D = 0.2634$), the energy consumption calculated as per standard is higher than for the other locations where F_D is approximately the same and is around 0.209, even though Athens benefits from the highest luminous exposure, see Table A.1.

This observation along with the LENI evaluation in Fig. 14 raises the question of whether the standard's tables for the evaluation of the daylight supply factor are reliable for southern latitudes.

4.2.2. Bratislava

Fig. 16 presents the LENI evaluation for an office in Bratislava with a west facade WWR of 0.2.

The largest discrepancies are observed for a south facade WWR of 0.1 and 0.7.

For WWR = 0.7, the discrepancies are due to the different treatment of light coming from the part of the window below the task area, see Fig. 10 and the respective explanation in Section 4.1.

For WWR = 0.1 and a high number of windows, one issue is the standard's calculation of the overall DF by superposition of the DFs for overlapping daylit areas, see Figs. 12 and 13 and the respective explanation in Section 4.1. However, discrepancies persist for a smaller number of windows where the standard's superposition approach is applicable. These may be due to the standard being optimized for code-compliant design and rooms with reasonable WWRs and WFRs. For example, for mixed-use spaces, a WFR of at least 0.1 may be prescribed [59]. Our office geometry with a south facade WWR of 0.1 has a WFR of 0.039 and thus does not comply with this limit.

For a south facade WWR of 0.5, the standard slightly overestimates

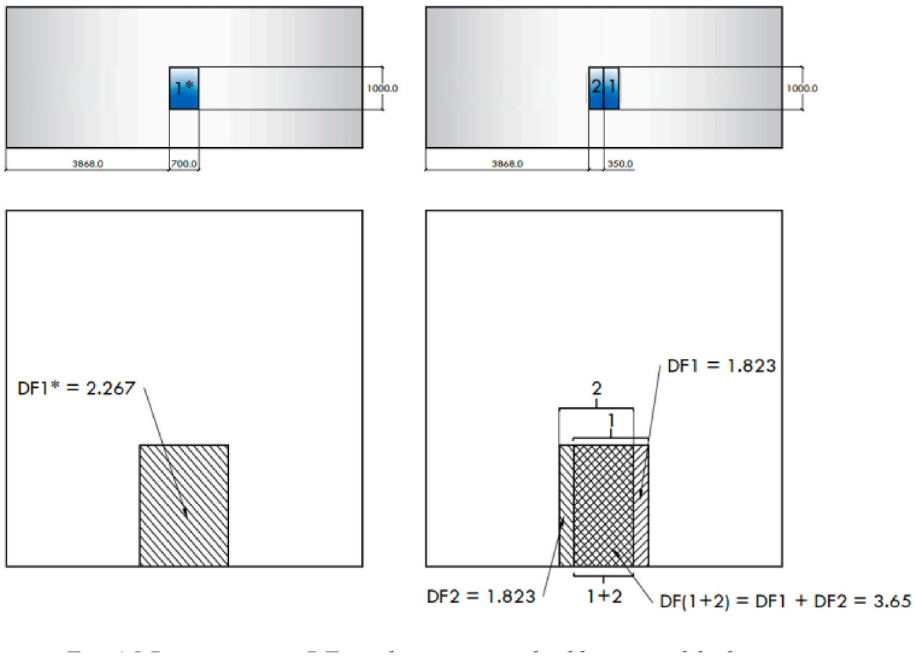

Fig. 13. Discrepancy in DF results as per standard because of daylit area superposition.

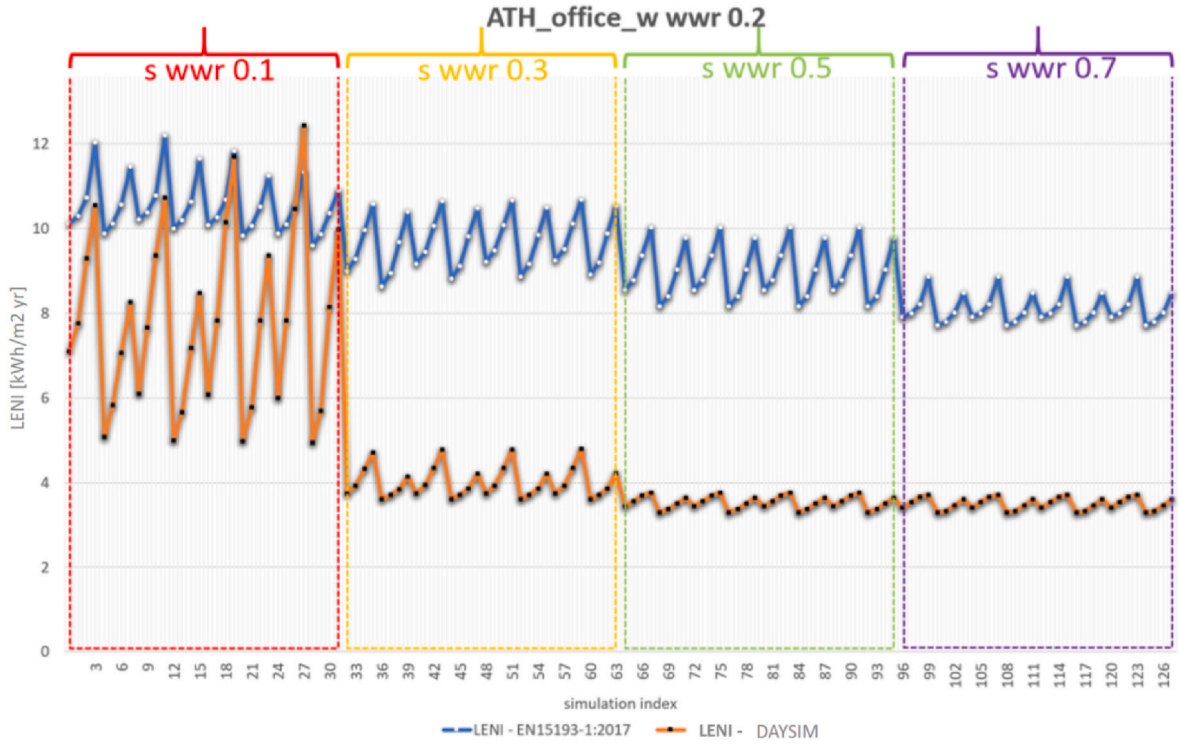

Fig. 14. LENI evaluation for an office in Athens with a west facade WWR of 0.2.

the LENI (compared with the DAYSIM calculation), especially in those cases without overhang. For a south facade WWR of 0.3, the standard slightly underestimates the LENI in the cases with overhang.

4.2.3. Stockholm

Fig. 17 shows that the LENI calculation for Stockholm as per standard is less accurate than for Bratislava. We investigate the reasons for this difference in accuracy between the two locations in the following.

Apart from the different daylight times t_D and daylight absence times t_N for Stockholm and Bratislava listed in Table 7, the daylight dependency factor F_D (calculated from the daylight supply factor $F_{D,S}$, see Eq. (A.8)) is the only factor in the LENI calculation that depends on location. Among all considered factors, latitude affects $F_{D,S}$ the most. However, the standard gives the same tabulated values for $F_{D,S}$ for Stockholm (latitude: 59°) and Bratislava (latitude: 48°) because both cities pertain to the latitude range of 45°–60° (see Table A.1). This is why the daylight dependency factor F_D is almost the same for both locations (see Table 8) in the example calculation in Section 4.2.1. We

			DF [%]									
γ	E_m [lx]	H_{dir}/H_{glob}	0.125	0.5	1	1.5	2	3	5	8	12	18
30°-45°	100	0.45	26.9	80.6	88.7	92.1	90.7	93	93.1	94.5	94.7	95.1
		0.71	17.8	53.3	70.1	80	78.4	84.6	85.6	89.5	90.3	90.9
	300	0.45	20.8	62.5	75.4	84.2	83.2	88.4	89.6	92.4	93.3	93.8
		0.71	10.8	32.3	46.6	57.1	56.8	66.4	70	77	82.4	83.6
	500	0.45	15.4	46.3	62.5	76	76.2	83.4	86.1	90.4	91.8	92.4
		0.71	7.6	22.8	36.4	46.6	46.2	55.3	59.5	67.8	73.6	75.4
	750	0.45	10.8	32.3	48.2	65.3	67.1	77.1	81.3	87.2	89.7	90.4
		0.71	5.3	16	27.8	38.2	38.2	47.1	51.3	59.6	65.9	68.2
	1000	0.45	8.3	24.9	37.7	55.4	58.3	71	77.2	84.6	87.8	88.6
		0.71	4.1	12.4	21.9	32	32.5	41.5	46	54.2	60.3	63

Fig. 15. Table for $F_{D,S,SNA,j}$ in the standard and relevant ranges for an example calculation.

Table 8
Variation of $F_{D,S,SNA,j}$ by location for the discussed case.

Location	$F_{D,S,SNA,j}$
Athens [GR]	73.66
Bratislava [SK]	79.08
Stockholm [SE]	79.06
London [GB]	79.04

Table 9
Daylight dependency factor F_D by location for the example calculation.

Location	F_D
Athens [GR]	0.2634
Bratislava [SK]	0.2092
Stockholm [SE]	0.2094
London [GB]	0.2096

conclude that the tabulated values for $F_{D,S}$ must be less appropriate for Stockholm than for Bratislava and lead to an overestimated daylight dependency factor and therefore an underestimated LENI.

4.2.4. *Effect of the overhang and overall LENI evaluation*

As reported in the previous sections, discrepancies were found to be larger in the presence of an overhang. Fig. 18 shows the LENI distribution calculated as per standard and with DAYSIM where cases were grouped by the presence or not of the overhang. Excluded were simulations for Athens and south facade WWRs of 0.1 and 0.7 because for these cases the standard's calculation presented issues that would confound the effect of the overhang as demonstrated in the previous sections.

Unsurprisingly, the presence of the overhang generally leads to an increase of the LENI, which is more pronounced in absolute value for the cases with a high LENI.

Compared with DAYSIM, the standard's calculation tends to underestimate the LENI in most cases except those with the lowest LENI values. This observation is in line with the conclusions made in the previous sections.

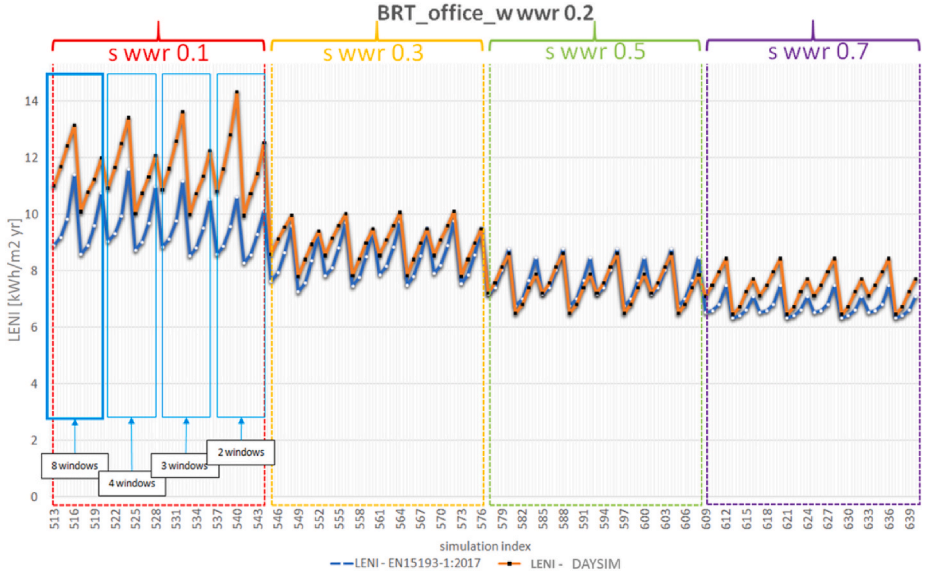

Fig. 16. LENI evaluation of an office in Bratislava with a west façade opening and varying south facade WWR.

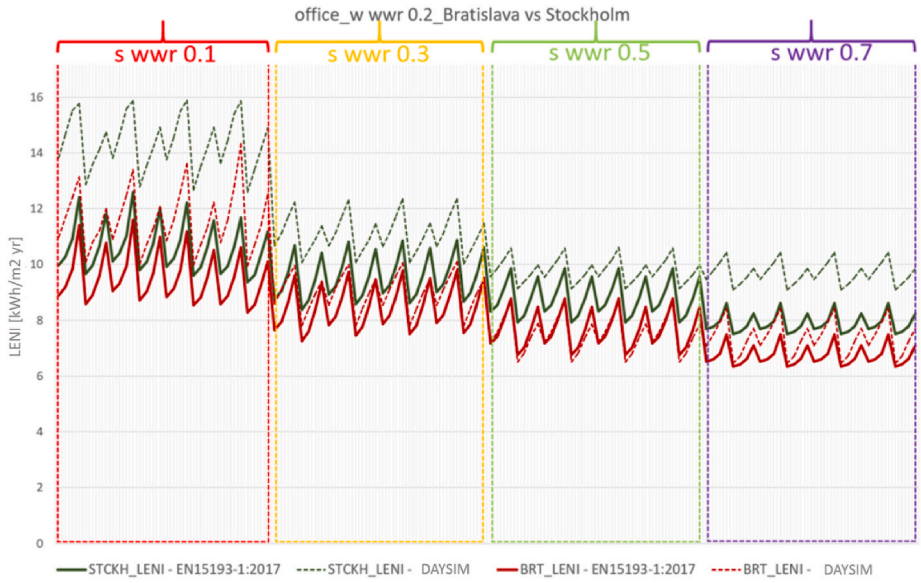

Fig. 17. LENI evaluation comparing an office with west opening and varying south facade WWR in Bratislava and Stockholm.

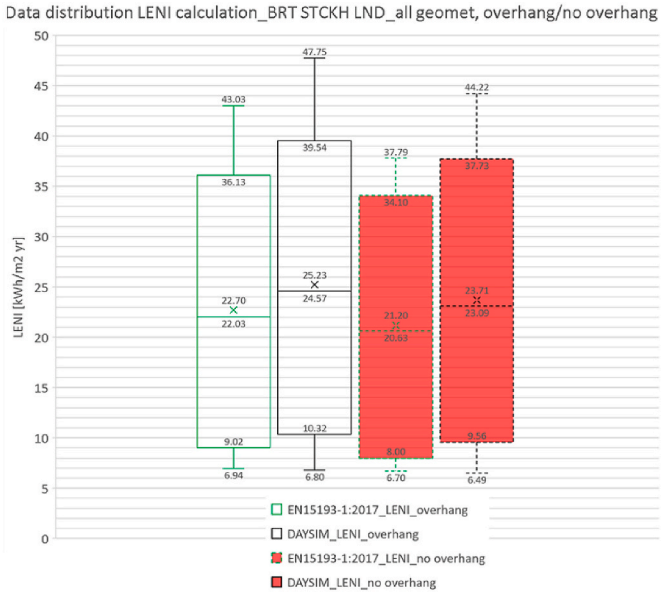

Fig. 18. LENI distributions grouped by presence or absence of overhang excluding Athens and south facade WWRs of 0.1 and 0.7.

5. Conclusions

This study presented an evaluation of the LENI and DF calculation according to standard EN15193-1:2017 against simulations performed in the Radiance-based software DAYSIM. In a full-factorial parametric analysis we assessed results for four locations across Europe, two room types (office and living room), 16 window configurations on the south façade for living room and 10 for office, an optional side opening on the west facade, two types of glazing (double or triple) and four overhang configurations, for a total of 1668 cases.

In the following, we summarize the issues found in the standard's calculations and provide suggestions for improvements. This assessment then allows us to report the range of applicability of the standard.

5.1. Summary of validation investigation, suggestions for improvement

1. For rooms with low WFR and WWR the standard's calculation is inaccurate.
2. In the DF calculation, the standard does not consider the windowsill level but only the window area. Thus, the standard cannot discern whether the task area is situated above or below the windowsill. However, this is crucial knowledge to adequately determine the illuminance over the task plane. By directly adding the contribution of direct light from the part of the window below the task plane to the illuminance on the task plane, the standard overestimates the DF and therefore underestimates the LENI.
3. For a high number of windows close to each other, the standard's approach to superpose the DFs for overlapping daylit areas leads to an overestimated DF and therefore an underestimated LENI.
4. The values for the daylight supply factor tabulated in the standard appear to be too low for latitudes below 45°. This leads to an overestimation of the LENI.
5. For latitudes above 60°, the daylight supply factor reported in the standard appears to be overestimated, which leads to an underestimation of the LENI.

To address the first two issues, our suggestion is to use Radiance or other validated tools instead of the standard for the calculation of the DF whenever several windows extend below the task plane or are close to each other. Further research is needed to identify suitable quantitative criteria. To address the third issue, a lower limit on WFR should be introduced into the next version of the standard. Possible thresholds are found in design codes. The fourth and fifth issues could be fixed by revising the respective tables in the standard.

Results for Bratislava and London demonstrate that the standard's calculation is adequate for locations in central Europe (i.e., latitudes between 45° and 60°). In this range, the standard's calculation is more consistent with DAYSIM results for cases with higher DF and therefore lower LENI. The LENI is also more consistent in cases with a side opening (which leads to a higher DF).

As a general conclusion, the standard tends to underestimate the LENI except for the case of Athens with the lowest LENI values. The underestimation is more pronounced for higher values of the LENI. Practitioners should keep this in mind when applying the standard, especially because they might improperly assume that a simplified procedure such as the one proposed by the standard would overestimate

the LENI to provide a conservative result.

5.2. Scope of applicability

It can be concluded: to obtain results of better reliability, it is suggested to apply the EN15193-1:2017 approach to spaces designed in the central European locations (latitudes within the range of 45°–60° with higher values of luminous exposure – around 0.5), with WWR's modeled in the range 0.3–0.5, keeping in the account that the sill level of openings is above the task area. The better results are achieved in cases where more than one façade has openings on it – due to daylight supply factor estimation tables.

In this sense, the addition of shading device of various size and form along with linear obstructions, as well as the reduction of visible transmittance values due to the use of different glazing typologies, and all the other factors that may influence the daylight penetration within the building, can contribute to the underestimation of LENI results with a different sensibility. Generally, the bigger the parameter change affects the DF results, the lower is the reliability of LENI results.

In the authors' opinion, it is important to keep in mind that generally, EN15193-1:2017 tends to underestimate LENI results.

Authors statement

Luka Akimov: Conceptualization, Methodology, Software, Validation, Writing- Original draft preparation, Visualization, Investigation, Writing- Reviewing and Editing.

Giuseppe De Michele: Methodology, Software, Validation, Resources, Supervision.

Ulrich Filippi Oberegger: Methodology, Writing- Reviewing and Editing, Validation, Supervision.

Vladimir Badenko: Supervision.

Andrea Giovanni Mainini: Methodology, Writing- Original draft preparation, Writing- Reviewing and Editing, Validation, Resources, Supervision.

Declaration of competing interest

The authors declare that they have no known competing financial interests or personal relationships that could have appeared to influence the work reported in this paper.

Acknowledgements

The authors thank the Department of Innovation, Research and University of the Autonomous Province of Bozen/Bolzano for covering the Open Access publication costs.

The research is partially funded by the Ministry of Science and Higher Education of the Russian Federation as part of World-class Research Center program: Advanced Digital Technologies [contract number 075-15-2020-934 dated 17.11.2020].

The authors would like to acknowledge the use of internal funding from EURAC Research for the research group Energy Efficient Buildings.

The authors would also like to thank Seed Lab.ABC, Politecnico di Milano for the support and assistance provided.

Appendix. [5]

A.1. Locations listed in the standard

Table A.1
Locations listed in the standard and used in the simulations

Location	Latitude γ [°]	Longitude ϕ [°]	Luminous exposure H_{dir}/H_{glob}
Athens, GR	*37.9*	*−23.7*	*0.56*
Bratislava, SK	*48.2*	*−17.2*	*0.46*
Stockholm, SE	*59.7*	*−18.0*	*0.42*
London, GB	*51.2*	*−0.2*	*0.39*

A.2. Summary of the standard's LENI calculation

The total required lighting energy in a zone of the building for a period t is estimated by:

$$W_t = \mathrm{W}_{L,t} + \mathrm{W}_{P,t}[kWh / t_s] \tag{A.1}$$

$\mathrm{W}_{L,t}$ is the lighting energy required to provide the designated illuminance level:

$$W_{L,t} = \sum\{(P_n \times F_c) \times F_o[(t_D \times F_D) + t_N]\} \Big/ 1000[kW / t_s] \tag{A.2}$$

t_D is daylight time when lighting could be possibly used and t_N is daylight absence time. Both depend on the occupancy schedule. P_n is the budget power installed [W], which depends on the power density of the luminaire and area of the building, its calculation is given below. F_c is the constant illuminance dependency factor, which depends on the maintenance factor and the efficiency factor of the constant illuminance control. F_o is the occupancy dependency factor, which depends on the absence factor, i.e. the proportion of time that the space is empty. F_D is the daylight dependency factor, which depends on the daylight availability. F_D is a function of the building's geometry along with the geometry of the openings, presence of obstructions, presence of shading devices, glazing properties etc.

The budget power installed is calculated as follows:

$$P_n = \mathrm{P}_j \times A\ [W] \tag{A.3}$$

Where A is the relevant area in the building [m^2];

P_j is the power density of the lighting:

$$P_j = \mathrm{P}_{j,lx} \times E_m \times F_{MF} \times F_{CA} \times F_L \left[W / m^2\right] \tag{A.4}$$

$\mathrm{P}_{j,lx}$ is the power density per lux of the area [W/lm], which is a tabulated value that depends on the photometric distribution of the luminaires and the shape of the room that they are covering. E_m is the maintained illuminance that the lighting system will be designed to provide [lx]. F_{MF} is the correction factor to account for the maintenance factor MF that is used in the lighting system design. F_{CA} is the factor to account for the reduced power required if parts of the area are lit to a lower level, it equals to 1 if the full illuminance is required for the whole area. F_L is the correction factor to account for the efficiency of the lighting equipment that will be used in the lighting system and is tabulated in standard considering the type of luminaire used.

$\mathrm{W}_{P,t}$ is the estimated standby energy required during periods in which lighting is switched off to provide the charging energy for emergency lighting and activation energy for lighting controls in a zone of the building. For its estimation, see Ref. [5].

The LENI is established using:

$$\mathrm{LENI} = \frac{W}{A}\left[\mathrm{kW} / \left(\mathrm{m}^2 \times \mathrm{year}\right)\right] \tag{A.5}$$

Where

W is the total annual energy consumption for lighting in the building [kWh/year];
A is the total useful floor area of the building [m^2].

A.3. Summary of the standard's daylight dependency factor $\mathbf{F_D}$ calculation

On the basis of geometrical parameters of the space along with geometrical parameters of openings and contribution of shading devices, the daylight factor of the raw carcass opening is estimated according to:

$$D_{CA,j} = \left(4.13 + 20.0 \times I_{Tr,j} - 1.36 \times I_{RD,j}\right) I_{Sh,j}\ [\%] \tag{A.6}$$

Where $I_{Tr,j}$ is a transparency index:

$$I_{Tr,j} = \frac{A_{Ca}}{A_D} \tag{A.7}$$

A_{Ca} denotes the raw building carcass opening and A_D the daylit area (i.e., the area exposed to daylight.

$I_{RD,j}$ and $I_{Sh,j}$ denote the space depth and shading index, respectively.

After calculating the daylight factor, the daylight dependency factor $\mathrm{F_d}$ is estimated:

$$F_D = 1 - \left[\mathrm{F}_{D,S} \times F_{D,C}\right] \tag{A.8}$$

Where $\mathrm{F}_{D,S}$ is the daylight supply factor defined as:

$$F_{D,S,j} = t_{rel,D,SNA,j} \times F_{D,s,SNA,j} + t_{rel,D,SA,j} \times F_{D,s,SA,j} \tag{A.9}$$

Where

$t_{rel,D,SNA,j}$ is the relative portion of the total operating time during which the solar protection system is inactive, which is a function of latitude γ of the site and luminous exposure $\mathrm{H_{dir}}/\mathrm{H_{glob}}$ representing the climate and façade orientation. The latter is tabulated in the standard.
$t_{rel,D,SA,j} = 1 - t_{rel,D,SNA}$ is the relative portion of the total operating time during which the solar protection system is active.
$F_{D,S,SNA,j}$ is the daylight supply factor of the area j evaluated whenever the solar protection system is inactive. It depends on latitude γ, luminous exposure $\mathrm{H_{dir}}/\mathrm{H_{glob}}$, façade orientation, level of maintained illuminance and daylight factor and is tabulated in the standard.
$F_{D,S,SA,j}$ is the daylight supply factor of the area j evaluated whenever the solar protection system is active. It depends on the solar protection system and is tabulated in the standard.
$F_{D,C}$ is a correction factor for daylight responsive control and depends on the control involved, daylight factor classification of the zone and the maintained illuminance level.

References

[1] M. Krarti, Energy Audit of Building Systems: an Engineering Approach, second ed., CRC Press, 2016.
[2] H. Poirazis, Å. Blomsterberg, M. Wall, Energy simulations for glazed office buildings in Sweden, Energy Build. 40 (2008) 1161–1170, https://doi.org/10.1016/j.enbuild.2007.10.011.
[3] P. Enkvist, T. Nauclér, J. Rosander, A cost curve for greenhouse gas reduction, McKinsey Q. 1 (34) (2007) 35–45.
[4] A.A. Baloch, P.H. Shaikh, F. Shaikh, Z.H. Leghari, N.H. Mirjat, M.A. Uqaili, Simulation tools application for artificial lighting in buildings, Renew. Sustain. Energy Rev. 82 (2018) 3007–3026, https://doi.org/10.1016/j.rser.2017.10.035.
[5] EN15193-1, Energy Performance of Buildings; Energy Requirements for Lighting, 2017.
[6] V.R.M. Lo Verso, G. Mutani, L. Blaso, A methodology to link the internal heat gains from lighting to the global consumption for the energy certification of buildings in Italy, J Daylighting 1 (2014) 56–67, https://doi.org/10.15627/jd.2014.6.
[7] F. Salata, A. De Lieto Vollaro, A. Ferraro, An economic perspective on the reliability of lighting systems in building with highly efficient energy: a case study, Energy Convers. Manag. 84 (2014) 623–632, https://doi.org/10.1016/j.enconman.2014.04.063.
[8] L. Martirano, A sample case of an advanced lighting system in a educational building, in: Int. Conf. Environ. Electr. Eng., EEEIC - Conf. Proc., IEEE Computer Society, Krakow, 2014, pp. 46–51, https://doi.org/10.1109/EEEIC.2014.6835834.
[9] E. Erkin, S. Onaygil, An approach for calculating lighting energy saving potentials in the office buildings on the basis of LENI data, Light Eng. 22 (2014) 37–46.

[10] D. Typańska, Ł. Putz, Analysis of the light and energy performance inside a lobby with an illumination made in LED technology, Przeglad Elektrotechniczny 90 (2014) 111–114, https://doi.org/10.12915/pe.2014.03.23.
[11] X. Yu, Y. Su, X. Chen, Application of RELUX simulation to investigate energy saving potential from daylighting in a new educational building in UK, Energy Build. 74 (2014) 191–202, https://doi.org/10.1016/j.enbuild.2014.01.024.
[12] C. Aghemo, L. Blaso, A. Pellegrino, Building automation and control systems: a case study to evaluate the energy and environmental performances of a lighting control system in offices, Autom. ConStruct. 43 (2014) 10–22, https://doi.org/10.1016/j.autcon.2014.02.015.
[13] A. Frattari, M. Chiogna, A. Mahdavi, Energetic implications of alternative lighting control strategies in an educational building, in: Sun, Wind Archit. - Proc. Int. Conf. Passive Low Energy Archit., PLEA, Singapore, 2007, pp. 149–154.
[14] L. Borowik, M. Kurkowski, Energy audit and energy consumption in interior lighting installations, Przeglad Elektrotechniczny 90 (2014) 285–287.
[15] C. Campanile, F. Leccese, M. Rocca, G. Salvadori, Energy saving exploiting light availability: a new method to evaluate daylight contribution, in: A. Gasparella, M. Baratieri, F. Patuzzi, V. Corrado (Eds.), Build. Simul. Appl, 2015– February, Free University of Bozen Bolzano, 2015, pp. 239–246.
[16] F.M. Raimondi, D. Curto, D. Milone, Environmental sustainability in non-residential buildings by automating and optimization LENI index, in: Int. Conf. Ecol. Veh. Renew. Energies, EVER, Institute of Electrical and Electronics Engineers Inc., 2018, pp. 1–6, https://doi.org/10.1109/EVER.2018.8362350.
[17] D. Typańska, T. Jarmuda, Improving the energy efficiency of lighting through the use of KNX system, Przeglad Elektrotechniczny 90 (2014) 80–83, https://doi.org/10.12915/pe.2014.07.15.
[18] T. Mjøs, P. Larsen, Indoor lighting - energy friendly installations, Light Eng. 20 (2012) 27–34.
[19] F.S. Yllmaz, A. Yener, Lighting energy performance determination for Turkey, Light. Res. Technol. 47 (2015) 740–759, https://doi.org/10.1177/1477153514541455.
[20] K.R. Wagiman, M.N. Abdullah, Lighting system design according to different standards in office building: a technical and economic evaluations, J. Phys. Conf. Ser. 1049 (2018), https://doi.org/10.1088/1742-6596/1049/1/012010. Institute of Physics Publishing.
[21] T. Novák, P. Bos, J. Šumpich, K. Sokanský, Statistical Evaluation of Dimmable Interior Lighting System Consumption Using Daylight, vol. 423, Springer Verlag, 2016.
[22] V.R.M. Lo Verso, A. Pellegrino, Energy saving generated through automatic lighting control systems according to the estimation method of the standard EN 15193-1, J Daylighting 6 (2019) 131–147, https://doi.org/10.15627/jd.2019.13.
[23] V.R.M. Lo Verso, A. Pellegrino, C. Aghemo, The Energy Performance for Lighting in Buildings According to the New en 15193-1: potential Energy Saving due to Different Photodimming Controls, in: Proc. - IEEE Int. Conf. Environ. Electr. Eng. IEEE Ind. Commer. Power Syst. Europe, EEEIC/I CPS Europe, Institute of Electrical and Electronics Engineers Inc., 2018, https://doi.org/10.1109/EEEIC.2018.8494448.
[24] DIAL GmbH, Manuale DIALux 9.1, 2020.
[25] LENICALC ENEA Official Web-site, 2020. https://www.pell.enea.it/lenicalc. (Accessed 4 October 2020).
[26] G. Parise, L. Martirano, L. Parise, A procedure to estimate the energy requirements for lighting, IEEE Trans. Ind. Appl. 2015 (2015), https://doi.org/10.1109/TIA.2015.2463761.
[27] A. Frattari, M. Chiogn, J. De Boer, Automation system for lighting control: comparison between data recorded and simulation model, Int. J. Hous. Sci. Appl. 33 (2009) 45–56.
[28] G. Parise, L. Martirano, G. Cecchini, Design and energetic analysis of an advanced control upgrading existing lighting systems, IEEE Trans. Ind. Appl. 50 (2014) 1338–1347, https://doi.org/10.1109/TIA.2013.2272752.
[29] G. Parise, L. Martirano, L. Parise, Energy performance of buildings: an useful procedure to estimate the impact of the lighting control systems, in: Conf. Rec. Ind. Commer. Power Syst. Tech. Conf, Institute of Electrical and Electronics Engineers Inc., Fort Worth, TX, 2014, https://doi.org/10.1109/ICPS.2014.6839154.
[30] R. Szczepaniak, W. Wilson, Investigating energy requirements for lighting: a critical approach to EN15193, in: Proc. Conf.: Adapt. Change: New Think. Comf, WINDSOR, Windsor, 2010.
[31] A. Tsangrassoulis, A. Kontadakis, L. Doulos, Assessing lighting energy saving potential from daylight harvesting in office buildings based on code compliance & simulation techniques: a comparison, Proc. Environ. Sci. 38 (2017) 420–427, https://doi.org/10.1016/j.proenv.2017.03.127.
[32] M. Tian, Y. Su, An improvement to calculation of lighting energy requirement in the European standard EN 15193:2007, J. Daylighting 1 (2014) 16–28, https://doi.org/10.15627/jd.2014.3.
[33] M. Zinzi, A. Mangione, The daylighting contribution in the electric lighting energy uses: EN standard and alternative method comparison, Energy Procedia 78 (2015) 2663–2668, https://doi.org/10.1016/j.egypro.2015.11.342.
[34] C. Aghemo, L. Blaso, S. Fumagalli, V.R.M.L. Verso, A. Pellegrino, The new prEN 15193-1 to calculate the energy requirements for lighting in buildings: comparison to the previous standard and sensitivity analysis on the new influencing factors, Energy Procedia 101 (2016) 232–239, https://doi.org/10.1016/j.egypro.2016.11.030.
[35] Maria Lo Verso, Valerio Roberto, Argun Paragamyan, Anna Pellegrino, Validation of the EN 15193:2017 calculation method to estimate the daylight supply in a building: comparison with dynamic climate-based simulations, in: 7th International Building Physics Conference, Syracuse, NY, USA, 2018, pp. 1037–1042, https://doi.org/10.14305/ibpc.2018.ms-2.06.
[36] DAYSIM Official Web-site, 2019. https://daysim.ning.com/. (Accessed 1 August 2018).
[37] Radiance Official Web-site, 2019. https://www.radiance-online.org/. (Accessed 1 August 2018).
[38] UNI 10840:2007: Luce e illuminazione - Localiscolastici - Criterigenerali per l'illuminazioneartificiale e naturale.
[39] IEA SHC Task 50, Advanced Lighting Solutions for Retrofitting Buildings, IEA Seminar, Rome, 12.6.2013.
[40] Energy Matching, Adaptive and Adaptable Envelope RES Solutions for Energy Harvesting to Optimize EU Building and District Load, 2019. https://www.energymatching.eu/. (Accessed 25 August 2018).
[41] CEN/TR 15193-2: Energy Performance of Buildings - Energy Requirements for Lighting - Part 2: Explanation and Justification of EN 15193-1, Module M9.
[42] M.I. Shamos, D. Hoey, Geometric intersection problems, in: 17th Annual Symposium on Foundations of Computer Science, Sfcs 1976), 1976, pp. 208–215, https://doi.org/10.1109/SFCS.1976.16.
[43] R. Athalye, H. Eckerlin, U. Atre, W.M. Street, Comparison of Results from the Daylighting Simulation of a Side-Lit Classroom Using Daysim with Actual Measured Annual Illuminances, (n.d.) vol. 8..
[44] C.F. Reinhart, S. Herkel, The simulation of annual daylight illuminance distributions—a state-of-the-art comparison of six RADIANCE-based methods, Energy Build. 32 (2) (2000) 167–187, https://doi.org/10.1016/S0378-7788(00)00042-6.
[45] J. Mardaljevic, Sky model blends for predicting internal illuminance: a comparison founded on the BRE-IDMP dataset, J. Build. Perform. Simulat. 1 (3) (2008) 163–173, https://doi.org/10.1080/19401490802419836.
[46] E. Brembilla, J. Mardaljevic, Climate-Based Daylight Modelling for compliance verification: benchmarking multiple state-of-the-art methods, Build. Environ. 158 (2019) 151–164, https://doi.org/10.1016/j.buildenv.2019.04.051.
[47] C.F. Reinhart, O. Walkenhorst, Validation of dynamic RADIANCE-based daylight simulations for a test office with external blinds, Energy Build. 33 (7) (2001) 683–697, https://doi.org/10.1016/S0378-7788(01)00058-5.
[48] Grasshopper, Algorithmic Modelling for Rhino, 2020. https://www.grasshopper3d.com/. (Accessed 30 July 2018).
[49] Rhinoceros Official Web-site, 2020. https://www.rhino3d.com/. (Accessed 1 August 2018).
[50] Ladybug Tools, 2020. https://www.ladybug.tools/. (Accessed 1 August 2018).
[51] EnergyPlus Official Web-site, 2020. https://energyplus.net/. (Accessed 30 July 2018).
[52] OpenStudio Official Web-site, 2020. https://www.openstudio.net. (Accessed 1 August 2018).
[53] Python Programming Language Official Web-site, 2020. https://www.python.org/. (Accessed 8 August 2018).
[54] G. Antonutto, A. McNeil, Radiance Primer. https://www.radiance-online.org/learning/tutorials/radiance-primer.pdf (accessed May 30, 2020).
[55] G. Ward, R. Shakespeare, Rendering with Radiance: the Art and Science of Lighting Visualization, 1998.
[56] C.F. Reinhart, J. Mardaljevic, Z. Rogers, Dynamic daylight performance metrics for sustainable building design, Leukos 3 (1) (2006) 7–31, https://doi.org/10.1582/LEUKOS.2006.03.01.001.
[57] Nutzungsbedingungen für die Energie – und Gebäudetechnik, SIA-Merkblatt 2024, Schweiz, Ing. & Srch.verein (SIA), Zürich, 2006.
[58] M.C. Peel, B.L. Finlayson, T.A. Mcmahon, Updated world map of the Köppen-Geiger climate classification, Hydrol. Earth Syst. Sci. Discuss. 4 (2007) 439–473, https://doi.org/10.5194/hess-11-1633-2007.
[59] Standard-Regolamento Edilizio BURL - Serie Avvisi e Concorsi - n. vol. 48 del 26.11.2014.